

A prediction-based reactive driving strategy for highly automated driving function on freeways

Mohammad Bahram¹, Anton Wolf¹, Michael Aeberhard¹ and Dirk Wollherr²

Abstract—Highly automated driving on freeways requires a complex artificial intelligence that makes optimal decisions based on the current measurements and information. The architecture of the decision-making process, hereinafter referred to as driving strategy, should allow diversity in decision-making for various traffic situations and modular expandability of the overall intelligence. Besides a reactive response to changes in the dynamic environment, a deliberative component should also be considered to incorporate the future evolution of the environment. This paper presents a novel driving strategy that meets the above requirements. The complex driving task is discretized by organization into a finite set of “behavioral strategies” through the developed “decision network”. The decision-making process itself is realized by a nonlinear model predictive approach which is solved using combinatorial optimization formulation. Lastly, the capability of the proposed approach is demonstrated in two freeway situations.

I. INTRODUCTION AND RELATED WORKS

The steady increase in the degree of automation can lead to improved traffic flow and reduced fuel consumption [1]. Advanced driver assistance systems (ADAS), such as adaptive cruise control and traffic jam assistant, are the most important examples of partially automated driving functions. Other ADAS, like forward collision warning, recognize specific hazardous situations faster than most human drivers, so that overall safety is significantly improved [1]. The highly automated driving function (HAD) represents the next higher level of automation. Since the 1990s, research is being conducted on various aspects of autonomous driving (see [2]–[9]). Driving on freeways with close-to-series sensors is one of the most challenging aspects of HAD. The main objective is to perform the complete driving task autonomously with maximum comfort. However, if a critical situation occurs, which can not be automatically resolved by the system, the driver must be brought back into the driving task within an appropriate time interval [10]. Through the use of HAD, the number of accidents caused by inattentive drivers in monotonous situations could be significantly reduced. Additionally, if the driver is no longer able to drive (e.g. due to a sudden heart attack), the function can completely take over the driving task and find a safe way to stop the car [11].

The driving strategy represents the artificial intelligence of the HAD system and performs the high-level decision-making process. In other words, it temporarily replaces

the decision-making of the human driver. Therefore, special requirements for the driving strategy must be derived. Modular expandability and transparency of the functional architecture enable future development of the system. The most determining requirement, however, is the safety for all traffic participants. For this reason, the decision-making process has to be controllable and robust. Besides reactivity, the evolution of traffic situations should also be considered in order to ensure a forward-looking driving behavior.

The functional architecture of the driving strategy is often realized by hierarchical finite state machines [4]–[6], [9]. This architecture has proven to be reliable. However, the state machine has to be designed such that the transparency of the system is guaranteed, even in complex traffic situations. The decision-making process can be realized either with rule-based [12] or utility-based [9], [13]–[15] algorithms. The advantages of the rule-based approach are simple implementation and traceability. However, the decision-making in complex traffic situations can not be modeled accurately enough. The approach based on the utility functions considers several criteria due to their weights. It can be extended relatively simple to complex scenarios. The disadvantage of this approach is, however, the large number of weighting parameters that are usually determined by trial and error tuning. Other approaches for the decision-making are based on fuzzy logic [16] and Bayesian networks [17]. These methods are less suitable when considering future events in the decision-making process. Another approach for the realization of the driving strategy module is based on the DAMN architecture [18]. Here, the driving behavior is determined by a fusion of multiple concurrent goals. Based on the situation awareness, the decision unit of the system finally makes direct decisions concerning driving maneuvers. Due to the fact that the fusion of concurrent goal has a direct influence on the conducted driving maneuvers, it causes traceability difficulties and a non-deterministic behavior [19].

This paper thus focuses on the driving strategy which meets the above-mentioned requirements. The main advances of the current work are on the one hand a well-organized functional architecture. Compared to [9], it meets a higher requirement of modular expandability. On the other hand, the decision-making process is based on a model predictive approach which enables the driving strategy to be reactive and to simultaneously consider the future evolution of the environment. In comparison to [9], [13], [20], a dynamic model is derived which predicts both the longitudinal and lateral maneuvers of all traffic participants. Furthermore, the combinatorial optimization formulation of the problem

¹M. Bahram, A. Wolf and M. Aeberhard are with BMW Group Research and Technology, D-80992 Munich, Germany emails: {mohammad.bahram, michael.aeberhard}@bmw.de; anton.wolf@tum.de

²D. Wollherr is with the Institute of Automatic Control Engineering of the Technische Universität München, D-80290 Munich, Germany email: dw@tum.de

always guarantees a solution within an appropriate computation time. Thus, the system robustness is given. Finally, the representative objective functions are organized in a priority-based approach in which the safety factor has the highest priority. A small number of parameters are tuned systematically using genetic algorithm.

This contribution is organized as follows: In Section II, the functional architecture of the driving strategy is presented. Section III discusses the model predictive decision-making process. Simulation results of the proposed algorithm are given in Section IV.

II. FUNCTIONAL ARCHITECTURE OF THE DRIVING STRATEGY

The entirety of the functional architecture is realized in a hierarchical decision network (Fig. 1). The complexity of the driving task is reduced by determining a discrete set of different behavioral strategies. Each behavior implements a suitable decision-making process for the specific traffic situation. The *Arbitration* activates the appropriate behavioral strategy based on the calculated features $\mathcal{F} \in \mathbb{R}^n$ and the dissatisfaction factor of the last active behavioral strategy $\delta \in \mathbb{R}$. This factor expresses the persistence of a non-optimal driving situation (e.g. lane change is desired but not possible). Therefore, the memory of the human driver is modeled too (the determination of δ is beyond the scope of this paper). This functional block is implemented by concurrent state machines due to the transparency requirement. The *Trajectory Planning* generates a set of collision-free trajectories with minimum jerk based on the various calculated driving goals [21].

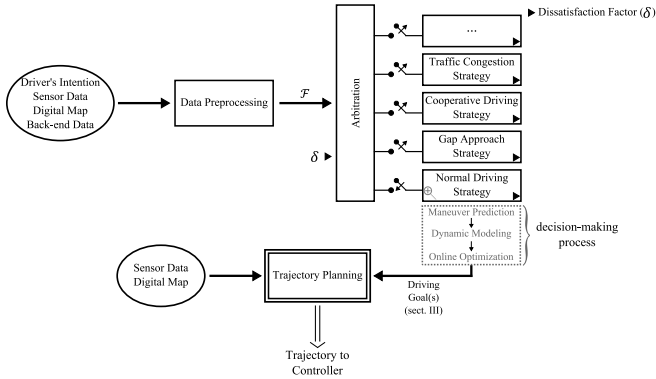


Fig. 1. Functional architecture: hierarchical decision network.

The functional architecture meets the requirements for modular expandability and transparency. Further improvements of the intelligence can be easily done by defining a new behavior and adapting the decision-making process to handle its specific requirements. Additionally, separation between the decision making process and the trajectory planning provides safety redundancy of the system.

The next section looks in detail at the model predictive decision making process of the *Normal Driving Strategy*, because this is active in most of the time. Although the

modular architecture of the decision network allows a differentiated decision-making process in each behavioral strategy, an adapted model predictive approach can be used for the other behaviors as well.

III. MODEL PREDICTIVE DECISION-MAKING PROCESS

Given the current sensor measurements, optimal decisions for further driving has to be determined. For this reason, a model predictive approach is derived which satisfies the two important requirements for reactivity and anticipatory [22]. It relies on a suitable dynamic model of the process. Therefore, at the k -th sampling time instance the state vector of the i -th vehicle $\mathbf{x}_{k+j|k}^i$ is predicted for the next p instances up to the prediction horizon H_p . The intervals in seconds between the prediction instances are given by

$$\Delta t_{pj} = \frac{j}{2}, j = 1, \dots, p \quad (1)$$

Due to the increase in uncertainty with a longer prediction time, the prediction intervals are increased linearly. For better clarity, the intervals in the following are drawn always equidistant. Subsequently a cost minimizing control strategy is computed for the fixed control horizon in the future $H_c \leq H_p$, taking into account the input and state constraints. Then the first step ($j = 1$) of the optimal policy sequence Π_k^* is implemented as the driving goal until the next sampling time instance $k + 1$. It defines the solution space of the subsequent trajectory planning

$$\Pi_k^* \in \mathbb{R}^{2 \times p} = \bigcup_{j=1}^p \pi_{k+j|k}^* \quad (2)$$

with its j -th elements

$$\begin{aligned} \pi_{1_{k+j|k}}^* &\in \mathbb{Z} = \{\pi_{1_{k+j|k}}^* \mid -1 \leq \pi_{1_{k+j|k}}^* \leq +1\} \\ \pi_{2_{k+j|k}}^* &\in \mathbb{R} = \{\pi_{2_{k+j|k}}^* \mid 0 \leq \pi_{2_{k+j|k}}^* \leq v_{\text{long,max}}\} \end{aligned}$$

where $\pi_{k+j|k}^*$ specifies the optimal maneuver at the corresponding prediction instance. $\pi_{1_{k+j|k}}^* = 0$ represents the lane keeping (LK) maneuver, whereas $\pi_{1_{k+j|k}}^* = \pm 1$ corresponds to the lane change right (LCR) resp. left (LCL) maneuvers. The optimal longitudinal target velocity $\pi_{2_{k+j|k}}^*$ is bounded to the upper limit of $v_{\text{long,max}}$. This itself is determined by the minimum of the driver's desired speed, road speed limits and comfortable speed in curves. At the next consecutive sampling time instance, the p -step policy is recalculated using the latest measurements. This procedure is repeated for an infinite sampling time instances (receding horizon approach). The main advantage of the model predictive decision-making process is the fact that it allows the current time slot to be optimized, while keeping account of future time slots. Additionally, it has the ability to anticipate future events and react accordingly. Through sufficiently rapid replanning, it is guaranteed that the cognitive vehicle responds to unforeseen events as well and, when necessary, abort the planned action.

For the model predictive decision-making a robust and computationally efficient maneuver prediction of all the traffic participants is required. For this reason, a suitable prediction model is derived in the next section.

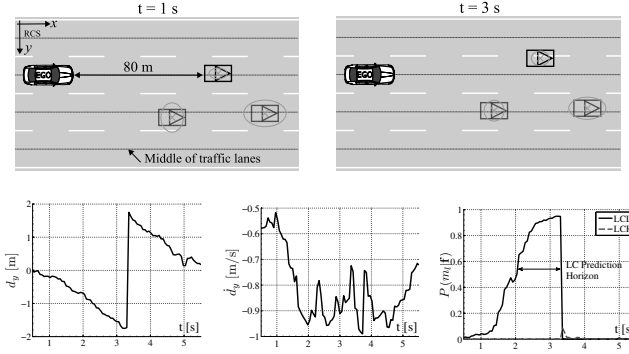


Fig. 2. Lane change prediction of the front vehicle (bold marked).

A. Maneuver Prediction and Dynamic Model

The longitudinal velocities of the other vehicles on free-ways can be assumed to be constant for the prediction horizon of $H_p \leq 3$ seconds. However, this assumption is not valid for the lateral direction, because the lane change intention and maneuver have a nonlinear behavior. Therefore, a separate prediction model is derived, which determines the maneuver intention (i.e. lane change probability) of the i -th vehicle at the current sampling time instance

$$I_{lc_k}^i \in [-1, 1] = \max_{m_l} [P(m_l | \mathbf{f}_k^i)] \text{sgn}(m_l) \quad (3)$$

with the three predefined maneuvers

$$m_l \in \mathbb{Z} = \{m_l | -1 \leq m_l \leq +1\} \triangleq \{\text{LCL}, \text{LK}, \text{LCR}\}$$

The feature vector of the i -th vehicle $\mathbf{f}_k^i \in \mathbb{R}^2 = \{d_y, \dot{d}_y\}$ represents its current measured trajectory. The lateral deviation d_y and lateral velocity \dot{d}_y are transformed to a lane-relative coordinate system, where the lateral origin is the middle of the lane (frenet coordinate system). This guarantees a correct prediction, even in curves. The lateral acceleration is neglected in favor of robustness. Additional conditionally independent features $\hat{\mathbf{f}} \in \mathbb{R}^n$ such as a turn signal and risk can be easily integrated. The maneuver prediction is based on the following Bayes classifier

$$P(m_l | \mathbf{f}, \hat{\mathbf{f}}) = \frac{P(d_y, \dot{d}_y | m_l) P(\hat{\mathbf{f}} | m_l) P(m_l)}{\sum_{L=1}^3 P(d_y, \dot{d}_y | m_L) P(\hat{\mathbf{f}} | m_L) P(m_L)} \quad (4)$$

The maneuver prediction model is trained based on the recorded data from real freeway traffic scenarios. The output of the model is shown in Fig. 2 for the front vehicle at a distance of about 80 meters. The bottom plots show its measured features and the lane change probability. This model is described in detail in [23]. In this contribution, only the expected values of the measurements and states are considered.

In order to assign objects to the lanes of the freeway, matching algorithms are required. Therefore, a road coordinate system (RCS) is defined and the state vector of each vehicle is transformed into it. In this system x represents the driven distance from the starting point of the road section and y the lateral distance from the leftmost lane marking.

The time-invariant nonlinear dynamic model of the traffic $g^{\text{TFC}} : \mathbb{R}^3 \times \mathbb{R}^2 \rightarrow \mathbb{R}^3$ determines the state vector $\mathbf{x}_{k+j|k}^i$ of the i -th vehicle for the next p prediction instances based on the Markov assumption

$$\mathbf{x}_{k+j|k}^i = g^{\text{TFC}}(\mathbf{x}_{k+j-1|k}^i, \mathbf{u}_k^i) \quad (5)$$

with the i -th vehicle's state vector in the RCS

$$\mathbf{x}_{k+j|k}^i \in \mathbb{R}^3 = \begin{pmatrix} x_{k+j|k}^i \\ y_{k+j|k}^i \\ v_{\text{long},k+j|k}^i \end{pmatrix} = \begin{pmatrix} \text{longitudinal position} \\ \text{lateral position} \\ \text{longitudinal velocity} \end{pmatrix}$$

and its measured control input vector at the current sampling time instance

$$\mathbf{u}_k^i \in \mathbb{R}^2 = \begin{pmatrix} I_{lc_k}^i \\ a_{\text{long},k}^i \end{pmatrix} = \begin{pmatrix} \text{maneuver intention} \\ \text{longitudinal acceleration} \end{pmatrix}$$

g^{TFC} can be described by the following system of equations (with constant velocity assumption, i.e. $a_{\text{long},k}^i = 0$)

$$\begin{aligned} x_{k+j|k}^i &= x_{k+j-1|k}^i + v_{\text{long},k+j-1|k}^i \Delta t_{p_j} \\ y_{k+j|k}^i &= y_{k+j-1|k}^i + \Delta y_{k+j|k}^i (I_{lc_k}^i) \\ v_{\text{long},k+j|k}^i &= v_{\text{long},k+j-1|k}^i \end{aligned} \quad (6)$$

Based on the predicted maneuver intention, an appropriate fifth-order polynomial trajectory for the i -th vehicle is generated and its lateral position along this trajectory at each prediction instance j is determined by $\Delta y_{k+j|k}^i (I_{lc_k}^i)$.

There is a reasonable simplification made by the traffic dynamic model: The predicted states of the i -th vehicle is decoupled from the policy of the ego vehicle at the specific prediction instance. This reduces the computational complexity of the subsequent optimization problem. This simplification is feasible, since the prediction horizon is small enough for neglecting interactions.

Because of the known ego policy at each prediction instance, the control input vector of the ego vehicle is defined as

$$\mathbf{u}_{k+j|k}^{\text{EGO}} \in \mathbf{u}_{k+j|k}^{\text{EGO}} \in \mathbb{R}^2 = \begin{pmatrix} \pi_{1,k+j|k} \\ \dot{\pi}_{2,k+j|k} \end{pmatrix}$$

$\mathbf{u}_{k+j|k}^{\text{EGO}}(\mathbf{x}_{k+j-1|k}^{\text{EGO}})$ determines the feasible solution space of the ego control input dependent on the previous ego state. The ego vehicle dynamics and other constraints are considered. The motion of the ego vehicle is predicted based on the constant acceleration assumption. Therefore, a different dynamic model $g^{\text{EGO}} : \mathbb{R}^3 \times \mathbb{R}^2 \rightarrow \mathbb{R}^3$ is derived which is described by the following system of equations

$$\begin{aligned} x_{k+j|k}^{\text{EGO}} &= x_{k+j-1|k}^{\text{EGO}} + v_{\text{long},k+j-1|k}^{\text{EGO}} \Delta t_{p_j} + \frac{\ddot{\pi}_{2,k+j-1|k} \Delta t_{p_j}^2}{2} \\ y_{k+j|k}^{\text{EGO}} &= y_{k+j-1|k}^{\text{EGO}} + \Delta y_{k+j|k}^{\text{EGO}}(\pi_{1,k+j|k}) \\ v_{\text{long},k+j|k}^{\text{EGO}} &= v_{\text{long},k+j-1|k}^{\text{EGO}} + \ddot{\pi}_{2,k+j-1|k} \Delta t_{p_j} \end{aligned} \quad (7)$$

where $\Delta y_{k+j|k}^{\text{EGO}}(\pi_{1,k+j|k})$ specifies the lateral position of the ego vehicle along the fifth-order polynomial trajectory dependent on the desired maneuver.

Based on the derived dynamic models, the evolution of the environment can be predicted. This is the precondition for the subsequent online dynamic optimization which is described in the next section. The modular architecture of the driving strategy allows the modification or defining new dynamic models for other behavioral strategies.

B. Discrete-Time Constrained Dynamic Optimization

The optimal policy sequence Π_k^* is computed by solving the following discrete-time constrained optimization problem

$$\min_{\pi_{k+j|k}} \left[\sum_{j=1}^p \Phi \left(\bigcup_i \mathbf{x}_{k+j|k}^i, \mathbf{x}_{k+j|k}^{\text{EGO}}, \pi_{k+j|k} \right) \lambda_j \right] \quad (8)$$

with respect to the constraints

$$\sum_{j=1}^p |\dot{\pi}_{1_{k+j|k}}| \leq 1 \quad (9)$$

$$a_{\text{decel,max}} = -4 \text{ m/s}^2 \leq \dot{\pi}_{2_{k+j|k}} \leq a_{\text{accel,max}} = 2 \text{ m/s}^2 \quad (10)$$

It is a cost-minimizing problem (with respect to the objective function $\Phi(\cdot)$) taking into account the derived dynamic models from III-A and the hard inequality constraints. The discount factor $\lambda_j \in]0, 1]$, $\lambda_{j+1} < \lambda_j$ considers the predicted costs with continuously falling weights in the overall optimization due to the increase of uncertainty in the prediction. In the lateral direction, the maximal number of lane changes is limited to one (9). The longitudinal vehicle dynamics with respect to the maximum acceleration and deceleration is limited by (10).

In order to guarantee a reactive behavior, the decision-making process has to be performed with a sampling period of at least $\Delta T = 0.2$ seconds [19]. Because of the nonlinearity in the dynamic model and objective function, a mixed integer nonlinear optimization problem has to be solved, which is in general computationally expensive. This class of optimization problems can be solved with different methods presented in [24]. However, another solution is discussed in the following.

The feasible solution space of the ego's control input $\mathcal{U}_{k+j|k}^{\text{EGO}}$ will be sufficiently fine discretized at each prediction instance. The problem can thus be viewed as a combinatorial optimization, searching for the best policy out of the discretized feasible solution space [25]. Depending on the discretization step size, the solution found is "sufficiently close" to the optimum. Subsequently the underlying trajectory planning guarantees a minimum jerk implementation of the driving goal.

For this reason, at each sampling time instance a weighted tree $T(V, E)$ is considered which is described by the two sets of vertices (nodes) V and edges E . The depth of each node corresponds to the specific prediction instance j . The edge weights represent their calculated costs. The problem is now reformulated in the well-known "single-source shortest path problem". In the following, the control horizon is limited to the prediction horizon (i.e. $H_c = H_p = 3$ seconds) and is divided into three instances (i.e. $p = 3$). The feasible

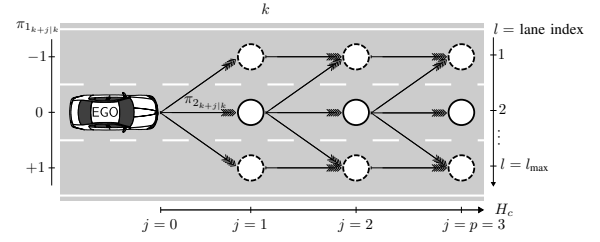


Fig. 3. Visualization of the search tree within the decision making process.

solution space of the ego's control input $\mathcal{U}_{k+j|k}^{\text{EGO}}$ for each of the three prediction instances $j = 1, 2, 3$ is discretized as follows: in the lateral direction the ego lane as well as lane change requests to the directly adjacent lanes (if they exist) is considered, taking into account the constrain from (9). In the longitudinal direction the velocity is discretized by a linearly spaced vector of seven values with respect to (10)

$$\pi_{2_{k+j|k}} = \pi_{2_{k+j-1|k}} + [-4 \text{ m/s}^2 : +1 : 2 \text{ m/s}^2] \Delta t_{p_j} \quad (11)$$

This results in a rooted search tree where each node has no more than $N = \min(3, l_{\text{max}}) \cdot 7$ children (with l_{max} = number of lanes). The variable N determines how accurate the discretization of the solution space is. Fig. 3 shows the introduced search tree for the sampling time instance k . The circles represent the set of all nodes at the j -th prediction instance. A distinction is made between the solid (continue on the same lane) and dashed nodes (with lane change request). The arrows illustrate the discretized velocities. The root node ($j = 0$) corresponds to the current measured state of the ego vehicle and the measured states and control inputs of surrounding traffic. Each other node represents a policy combination from the feasible solution space. In addition, it represents a separate data structure which stores, among others, the predicted state vectors and the accumulated cost from the root node along exactly one elementary path (because of the arborescence property of the tree). Finally the tree will be searched for the shortest path, i.e. the path with the lowest cost, by using the Dijkstra's algorithm [26]. When the ego vehicle is forced to merge into another lane as soon as possible (e.g. in freeway entrance), the best solution for the requested lane change direction can be also passed as a further driving goal to the trajectory planning. This shows the flexibility of the presented approach.

A complete overtaking maneuver is not considered due to the equation 9. Because such a maneuver requires a significantly large prediction horizon (i.e. $H_p \gg 3$ seconds). However, there is not a sufficiently accurate prediction model of the traffic for such a long time horizon. Furthermore the computational complexity rises polynomial with the discretization of the solution space N but exponential with the prediction instances p (i.e. $\mathcal{O}(N^p)$). Thus, planning over such a large prediction horizon, due to reasons of complexity, is limited.

The definition of suitable objective functions has a great influence on the safety and comfort of the driving strategy.

For this reason, a priority-based approach is discussed in detail in the next section. The goal is to define a set of representative functions with a minimal number of parameters.

C. Definition Of The Objective Function

A main issue in constrained problems is that they may get infeasible when disturbances occur. The idea to overcome this was to introduce a “level-based” objective function. The cost resulting from the objective function is sub-divided in 3 levels. The priority is ascending with the level number. This constraint softening approach guarantees, that the problem remains always feasible.

The level-3 cost takes account of the ego vehicle’s safety. For this purpose, a risk factor to the vehicles ahead is calculated based on time to collision (TTC) and intervehicular time (TIV). The time based on TTC controls the safety distance to all i cars dependent on the velocity difference

$$t_{\text{ttc},k+j|k}^i = \frac{x_{k+j|k}^i - x_{k+j|k}^{\text{EGO}}}{\pi_{2k+j|k} - v_{\text{long},k+j|k}^i} \quad (12)$$

The time based on TIV controls the safety distance to all i cars dependent on the ego velocity

$$t_{\text{tiv},k+j|k}^i = \frac{x_{k+j|k}^i - x_{k+j|k}^{\text{EGO}}}{\pi_{2k+j|k}} \quad (13)$$

The maximum risk is determined by the minimum time. Thus, the risk r for both the TTC time $t_{\text{ttc},k+j|k}^i = \min_i [t_{\text{ttc},k+j|k}^i]$ and TIV time $t_{\text{tiv},k+j|k}^i = \min_i [t_{\text{tiv},k+j|k}^i]$ is given by

$$r_{\text{ttc/tiv},k+j|k} = \begin{cases} 1, & \text{if } t_{\text{ttc/tiv},k+j|k} \leq t_{\text{ttc/tiv},\min} \\ 0, & \text{if } t_{\text{ttc/tiv},k+j|k} \geq t_{\text{ttc/tiv},\max} \\ 1 - \frac{t_{\text{ttc/tiv},k+j|k} - t_{\text{ttc/tiv},\min}}{t_{\text{ttc/tiv},\max} - t_{\text{ttc/tiv},\min}} \end{cases} \quad (14)$$

The accumulated level-3 cost along each n -th elementary path is

$$\begin{aligned} \Phi_{\text{L3},k,n} &\in [p+1, p+2] \\ &= p+2 - \prod_{j=1}^p [(1 - r_{\text{ttc},k+j|k,n}) (1 - r_{\text{tiv},k+j|k,n})] \end{aligned} \quad (15)$$

The level-2 cost considers the traffic laws. Initially only one of the key regulations for driving on Germany’s freeway, not overtaking on the right side, is implemented. For this reason, the front vehicle on the left adjacent lane $i = fl$ is taken into account. The idea is to project this vehicle on all lanes on its right side. Then the risk to collide with the projected vehicle based on TIV and TTC is calculated in the same way as for the level-3 cost. The accumulated level-2 cost along each n -th elementary path is

$$\begin{aligned} \Phi_{\text{L2},k,n} &\in [p, p+1] \\ &= p+1 - \prod_{j=1}^p [(1 - r_{\text{ttc},k+j|k,n}^{i=fl}) (1 - r_{\text{tiv},k+j|k,n}^{i=fl})] \end{aligned} \quad (16)$$

The level-1 cost represents the comfort. The accumulated level-1 cost along each n -th elementary path is

$$\begin{aligned} \Phi_{\text{L1},k,n} &\in [0, p] \\ &= \sum_{j=1}^p \left[\frac{(w_1 \phi_{1,k+j|k,n} + w_2 \phi_{2,k+j|k,n} + w_3 \phi_{3,k+j|k,n})}{w_1 + w_2 + w_3} \right] \end{aligned} \quad (17)$$

The ϕ_1 cost is dependent on the difference to the bounded desired speed $v_{\text{long},\max}$

$$\phi_{1,k+j|k,n} = 1 - \text{sech}(v_{\text{long},\max} - \pi_{2k+j|k,n}) \quad (18)$$

The ϕ_2 cost prefers free lanes. The cost of the desired lane is dependent on the distance to the leading car $d_{k+j|k,n}^{i=dl} = |x_{k+j|k,n}^{i=dl} - x_{k+j|k,n}^{\text{EGO}}|$ and the distances to the leading cars on all reachable lanes $i \in F_i$

$$\phi_{2,k+j|k,n} = \frac{\frac{1}{d_{k+j|k,n}^{i=dl}}}{\sum_{i \in F_i} \frac{1}{d_{k+j|k,n}^i}} \quad (19)$$

The ϕ_3 cost rewards driving on the rightmost lane $l_{\max,k}$

$$\phi_{3,k+j|k,n} = \frac{l_{\max,k} - l_{k+j|k,n}^{\text{EGO}} (y_{k+j|k,n}^{\text{EGO}})}{l_{\max,k} - 1} \quad (20)$$

Furthermore it must be guaranteed that paths with level-3 or level-2 cost are only taken, if there are no paths with level-1 cost:

$$\begin{aligned} \text{If } \Phi_{\text{L3},k,n} \geq p+1 & \quad \text{then } \Phi_{\text{L2},k,n} = \Phi_{\text{L1},k,n} = \infty \\ \text{If } \Phi_{\text{L2},k,n} \geq p & \quad \text{then } \Phi_{\text{L1},k,n} = \infty \end{aligned} \quad (21)$$

Finally, the path with the minimum cost is taken

$$\Phi_k^* = \min_n [\min [\Phi_{\text{L1},k,n}, \Phi_{\text{L2},k,n}, \Phi_{\text{L3},k,n}]] \quad (22)$$

This formulation guarantees that the problem is always feasible. Furthermore the ego vehicle would always prefer to take over a car on the left side. But when it is not possible, it would rather take over another car on the right side, than daring to collide with it. The weights w_1, w_2, w_3 were trained using a genetic algorithm based on natural selection [27].

The entire process flow of the driving strategy is given as an algorithm in the appendix.

IV. SIMULATION RESULTS

The functionality of the presented approach has been evaluated. For this purpose, a simulated environment was developed. This section first describes the implementation of the simulated environment, then the advantages of the prediction-based reactive driving strategy are demonstrated by two simulated freeway scenes.

The environment is developed for common and extreme freeway situations. Multiple parameters such as the number of lanes, the number of vehicles, or the duration of the simulation are adjustable. Different intelligent vehicles can be chosen. Vehicles without the possibility to change the lane (only longitudinal controller) are available as well as vehicles which have a longitudinal and lateral controller, but only with a reactive driving strategy. Lastly, vehicles with

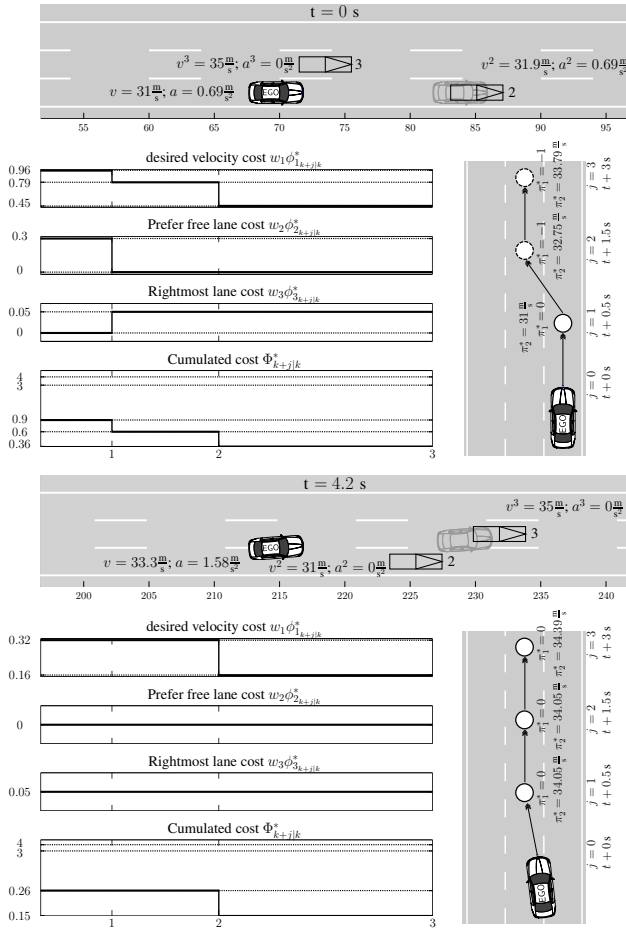


Fig. 4. Freeway situation 1: The ego vehicle takes over vehicle 2 after faster vehicle 3 passed.

the driving strategy described in Sections II and III can be chosen, e.g. the ego vehicles in the following examples.

To prove the functionality of the driving strategy, two freeway scenes were chosen. Fig. 4 and Fig. 5 provides two plots of moments of the scenes. Each plot visualizes the vehicles their current state. The diagrams below display the single costs of the path with the global minimum cumulated cost along the predicted steps. The first three charts illustrate the single level-1 criteria (18, 19 and 20). The last chart shows the cumulated cost (22). The optimal policy (i.e. the best path in the search tree) is also shown. Additional to the states of the vehicles at time t the state of the ego vehicle at time $t + \Delta t_{p_1}$ is visualized as a transparent car. Due to the time shift, the visualization of the positions of the other vehicles and the ego vehicle prediction have to be regarded with caution. I.e. the transparent car and the vehicles are not colliding.

In Fig. 4 the ego vehicle has a desired velocity of 35 m/s. But vehicle 2 only driving at 31 m/s with a constant acceleration of 0 m/s². At the same time vehicle 3 is nearly at the same longitudinal position on the adjacent lane of the ego vehicle and is driving faster. A rational human driver would wait until the faster vehicle 3 passed and would then take

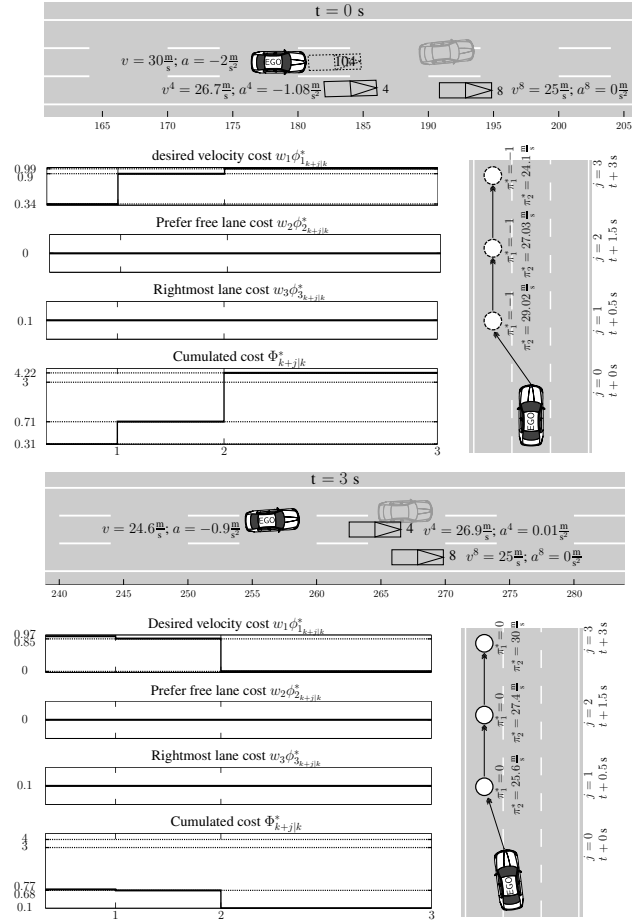


Fig. 5. Freeway situation 2: vehicle 4 cuts in close in front of the ego vehicle

over vehicle 2. In the first plot all policies which change the lane in the first prediction step have level-3 cost, because the ego vehicle would collide with vehicle 3. Therefore, a policy is chosen which makes the ego vehicle stay behind in the first prediction step and then begins the overtaking maneuver in the second prediction step after vehicle 3 has passed. This is reflected in the increasing ϕ_3 cost (ego vehicle is not on the rightmost lane anymore) and the decreasing ϕ_2 cost (there is no slower car on the middle lane). A few seconds later (see lower plot in Fig. 4) the ϕ_1 cost for driving the desired velocity decreases rapidly because the ego vehicle can drive faster on the free lane.

The initial state of the situation shown in Fig. 5 is that the ego vehicle approaches two vehicles on the right lane with a desired velocity of 30 m/s. Suddenly vehicle 4 changes to the middle lane just in front of the ego vehicle. If the ego vehicle keeps its velocity and lane, it would collide with vehicle 4. The upper plot shows that the maneuver prediction already recognized the lane change intention (see vehicle 104 with dashed line) even before vehicle 4 has reached the middle lane. The driving strategy chooses a policy with safety cost at the third prediction step, because at this moment each policy has safety cost due to the inevitable small distance to vehicle 4. The chosen policy reduces the velocity of the ego

vehicle (see increasing ϕ_1 cost) and initiates a lane change. The lower plot shows that the optimal policy is now not risky anymore because vehicle 4 is already driving faster than the ego vehicle.

The first scene demonstrates that the driving strategy chooses the most comfortable policy by consideration of the current situation (reactive). Moreover, the decision-making process based on the level-1 cost is coherent by taking a look at the single objectives (transparent and deterministic). The second scene proves that the driving strategy takes the future evolution of the environment into account (anticipating). Last it shows that in critical situations safe policies are favored over comfortable policies. Thus the prediction-based reactive driving strategy meets the requirements.

V. CONCLUSION

This paper presented a novel driving-strategy module which represents the artificial intelligence of the highly automated driving function. The advantage of this approach is that the driving strategy is modular expandable and transparent due to its functional architecture. The derived predictive decision-making process is both reactive and deliberative, allowing comfortable and safe driving for all the traffic participants. Additionally, the traffic rules are also considered. Due to the separation in levels, the approach allows a straightforward extension to additional costs. Flexibility and safety redundancy are two further advantages of the model.

APPENDIX

Algorithm Prediction-Based Reactive Driving Strategy

```

for  $k = 0$  to  $\infty$  do
  DATA-PREPROCESSING(.)
  ARBITRATION(.) # activate proper behavioral strategy
  for  $j = 1$  to  $p$  do
    for  $i = 1$  to  $N_{\text{CARS}}$  do
       $\mathbf{u}^{\text{TFC}}[i] \leftarrow \text{Measurements}$ 
       $\mathbf{x}^{\text{TFC}}[i][j] \leftarrow g^{\text{TFC}}(\mathbf{x}^{\text{TFC}}[i][j-1], \mathbf{u}^{\text{TFC}}[i])$ 
    end for
  end for
   $\text{tree} \leftarrow \text{EXPAND-TREE}(\cdot)$  # wrt. constraints
  for  $n = 1$  to  $N_{\text{NODES}}$  do
     $f \leftarrow \text{FATHER-NODE}(n)$ 
     $\pi \leftarrow \text{POLICY-VECTOR}(n)$ 
     $\mathbf{x}^{\text{EGO}}[n] \leftarrow g^{\text{EGO}}(\mathbf{x}^{\text{EGO}}[f], \pi)$ 
     $\Phi[n] \leftarrow \Phi(\mathbf{x}^{\text{TFC}}[n], \mathbf{x}^{\text{EGO}}[n], \pi)$ 
  end for
   $\Pi_k^* \leftarrow \text{DIJKSTRA-SEARCH}(\text{tree})$ 
end for

```

REFERENCES

- [1] M. Benmimoun, A. Pütz, A. Zlocki, and L. Eckstein, "Effects of acc and faw on speed, fuel consumption, and driving safety," in *Vehicular Technology Conference (VTC Fall)*, 2012 IEEE, 2012, pp. 1–6.
- [2] H.-H. Nagel, *Informatikforschung in Deutschland*. Springer, 2008, ch. EUREKA-Projekt PROMETHEUS und PRO-ART, pp. 151–166.
- [3] Thrun *et al.*, "Stanley: The robot that won the darpa grand challenge," *Journal of Field Robotics*, vol. 23, no. 9, pp. 661–692, 2006. [Online]. Available: <http://dx.doi.org/10.1002/rob.20147>
- [4] S. Kammel *et al.*, "Team annieway's autonomous system for the 2007 darpa urban challenge," *Journal of Field Robotics*, vol. 25, no. 9, pp. 615–639, 2008.
- [5] Urmson *et al.*, "Autonomous driving in urban environments: Boss and the urban challenge," *Journal of Field Robotics*, vol. 25, no. 8, pp. 425–466, 2008.
- [6] M. Montemerlo *et al.*, "Junior: The stanford entry in the urban challenge," *J. Field Robot.*, vol. 25, no. 9, pp. 569–597, Sept. 2008.
- [7] S. Thrun and C. Urmson, "How google's self-driving car works," <http://spectrum.ieee.org/automaton/robotics/artificial-intelligence/how-google-self-driving-car-works>, IEEE Spectrum, [Online; accessed 22-August-2013].
- [8] F. Saust, J. M. Wille, B. Lichte, and M. Maurer, "Autonomous vehicle guidance on braunschweigs inner ring road within the stadtpilot project," *IEEE Intelligent Vehicles Symposium*, pp. 169–174, 2011.
- [9] M. Ardelet, C. Coester, and N. Kämpchen, "Highly automated driving on freeways in real traffic using a probabilistic framework," *Intelligent Transportation Systems, IEEE Transactions on*, vol. 13, pp. 1576–1585, 2012.
- [10] C. Gold, D. Damböck, L. Lorenz, and K. Bengler, "'Take Over!'" How long does it take to get the driver back into the loop?" in *57th Human Factors and Ergonomics Society (HFES) International Annual Meeting*, San Diego (CA), USA, September 2013.
- [11] N. Kaempchen, M. Aeberhard, P. Waldmann, M. Ardelet, and S. Rauch, "Der bmw nothalteassistent: Hochautomatisiertes fahren für mehr sicherheit im straßenverkehr," *Elektronik Automotive*, vol. 8/9, pp. 26–29, September 2011.
- [12] C. R. Baker and J. M. Dolan, "Traffic interaction in the urban challenge: Putting boss on its best behavior," *IEEE/RSJ International Conference on Intelligent Robots and Systems*, pp. 1752–1758, September 2008.
- [13] J. Wei, J. M. Dolan, and B. Litkouhi, "A prediction- and cost function-based algorithm for robust autonomous freeway driving," in *IEEE Intelligent Vehicles Symposium*, Juni 2010, pp. 512–517.
- [14] A. Furda and L. Vlacic, "Enabling safe autonomous driving in real-world city traffic using multiple criteria decision making," *Intelligent Transportation Systems Magazine, IEEE*, vol. 3, no. 1, pp. 4–17, 2011.
- [15] D. C. K. Ngai and N. H. C. Yung, "A multiple-goal reinforcement learning method for complex vehicle overtaking maneuvers," *Intelligent Transportation Systems, IEEE Transactions on*, vol. 12, no. 2, pp. 509–522, 2011.
- [16] M. Pellkofer, "Verhaltensentscheidung für autonome fahrzeuge mit blickrichtungssteuerung," Ph.D. dissertation, Universität der Bundeswehr München, 2003.
- [17] J. H. Schneider, "Modellierung und erkenntung von fahrsituationen und fahrmanövern für sicherheitsrelevante fahrerassistenzsysteme," Ph.D. dissertation, Technischen Universität Chemnitz, 2009.
- [18] Rauskolb *et al.*, "Caroline: An autonomously driving vehicle for urban environments," *Journal of Field Robotics*, vol. 25, no. 9, pp. 674–724, 2008.
- [19] M. Ardelet, "Hybrid control strategies for advanced safety- and driver assistance systems," Ph.D. dissertation, München, Technische Universität, 2012.
- [20] J. Nilsson and J. Sjöberg, "Strategic decision making for automated driving on two-lane, one way roads using model predictive control," in *Intelligent Vehicles Symposium*, 2013.
- [21] M. Werling, S. Kammel, J. Ziegler, and L. Gröll, "Optimal trajectories for time-critical street scenarios using discretized terminal manifolds," *The International Journal of Robotics Research*, vol. 31, no. 3, pp. 346–359, 2012.
- [22] J. Maciejowski, *Predictive Control with Constraints*. Prentice Hall, 2002.
- [23] M. Bahram, A. Lohrer, and M. Aeberhard, "Generatives prädiktionsmodell zur frühzeitigen spurwechselerkennung," in *9. FAS-Workshop Fahrerassistenzsysteme Walting*, 2014, to be published.
- [24] J. Lee and S. Leyffer, Eds., *Mixed Integer Nonlinear Programming*. Springer, 2012.
- [25] M. Papageorgiou, M. Leibold, and M. Buss, *Optimierung. Statische, dynamische, stochastische Verfahren für die Anwendung*. Springer Vieweg, 2012.
- [26] T. H. Cormen, C. E. Leiserson, R. L. Rivest, and C. Stein, *Introduction to Algorithms*. The MIT Press, 2009.
- [27] A. E. Eiben and J. E. Smith, *Introduction to Evolutionary Computing*. Springer, 2007.